Japanese Journal of Radiology (2019) 37:336–340
https://doi.org/10.1007/s11604-019-00812-8

ORIGINAL ARTICLE

Differences in gross tumor volumes for pancreatic cancer: a comparison of ungated positron emission tomography and contrast-enhanced four-dimensional computed tomography

Shigeo Takahashi[1] · Masahide Anada[1] · Toshifumi Kinoshita[1] · Takamasa Nishide[1] · Toru Shibata[1]

Received: 11 October 2018 / Accepted: 16 January 2019 / Published online: 24 January 2019

Abstract

Purpose We assessed differences in gross tumor volumes (GTVs) for pancreatic cancer between respiratory-ungated positron emission tomography (3D-PET) and contrast-enhanced four-dimensional computed tomography (CE-4DCT).

Materials and methods We evaluated the GTVs in 21 patients. The sum of the GTVs, which was individually delineated by observers 1 and 2 on the CE-4DCT images from all respiratory phases, was used as GTV-4DCT. The GTVs on the 3D-PET images were extracted with three thresholds: 20%, 30%, and 40% of maximum activity concentration (GTV-*n*%). We selected one of the GTV-*n*%, which mostly resembled GTV-4DCT in size, as GTV-PET. Differences in the GTVs were analyzed.

Results Median values of GTV-4DCT for observers 1, 2, and GTV-PET were 55.0 mL, 45.7 mL, and 14.6 mL, respectively. GTV-PET was smaller than GTV-4DCT for observers 1 and 2 ($p < 0.01$ each). Differences of median values of maximum diameters between GTV-4DCT and GTV-PET were 1.7–1.8 cm, 1.4–1.6 cm, and 1.9–2.1 cm in the left–right, anterior–posterior, and craniocaudal directions, respectively.

Conclusion GTV-PET based on 3D-PET images was smaller than GTV-4DCT for pancreatic cancer. When we refer to 3D-PET images without CE-4DCT images, we need to pay attention to the above-mentioned finding to contour the GTV.

Keywords Delineation · Contouring · Ungated · 3D-PET · 4D-CT

Introduction

In the clinical practice of pancreatic cancer, fluorodeoxyglucose (FDG) positron emission tomography (PET) is helpful to detect tumors not only for the purpose of diagnosis [1] but also for radiation treatment planning [2]. A conventional respiratory-ungated PET (3D-PET) scan is acquired between 2 and 5 min duration with the patient breathing freely, and the FDG-avid lesion becomes blurred by respiratory motion [3]. Recently, the usefulness of respiratory-gated PET (4D-PET) in the radiation treatment planning for pancreatic cancer has been reported; the target volumes generated from 4D-PET were more accurate than those from 3D-PET [4]. However, a 4D-PET scan requires additional equipment such as a respiratory monitoring system and advanced display software, which are not available in all institutions [3]. Therefore, in the present study, we used conventional 3D-PET.

A 3D-PET scan includes the influence of respiratory motion [3]. In radiation treatment planning, to measure the respiratory motion, four-dimensional computed tomography (4DCT) is usually used. The comparison of the gross tumor volume (GTV) delineation of pancreatic cancer between 3D-PET and 4DCT has been reported [5]. In the study, GTVs based on the 4DCT images were contoured with 3 of 10 respiratory phases, and all of the respiratory motion was not included.

✉ Shigeo Takahashi
shigeot@med.kagawa-u.ac.jp

Masahide Anada
anada-m@med.kagawa-u.ac.jp

Toshifumi Kinoshita
kanikoro_taym_8361@yahoo.co.jp

Takamasa Nishide
tnishide@med.kagawa-u.ac.jp

Toru Shibata
tshibata@med.kagawa-u.ac.jp

[1] Department of Radiation Oncology, Kagawa University Hospital, 1750-1 Ikenobe, Miki-Cho, Kita-Gun, Kagawa 761-0793, Japan

In our institution, the GTVs are generated from all respiratory phases on contrast–enhanced 4DCT (CE-4DCT) images. Therefore, as the volumes include the respiratory motion, we conducted the present study to assess the differences in the GTVs for pancreatic cancer between 3D-PET and CE-4DCT with all respiratory phases.

Table 1 Patient and tumor characteristics

Characteristics		%
Sex		
Male	9	43
Female	12	57
Age (years)		
Median	68	
Range	41–81	
Histology		
Adenocarcinoma	21	100
Tumor location		
Pancreatic head	18	86
Pancreatic body	3	14
TNM classification[a]		
cT1N0M0	1	5
cT2N0M0	1	5
cT3N0M0	16	75
cT3N1M0	1	5
cT3N1M1LYM[b]	1	5
cT4N0M0	1	5
SUVmax		
Median	7.6	
Range	3.6–17.1	

CE-4DCT contrast-enhanced 4-dimensional computed tomography, *3D-PET/CT* respiratory-ungated positron emission tomography/computed tomography, *FOV* field of view

[a]Seventh edition of the Union for International Cancer Control

[b]The patient had an abdominal aortic lymph node metastasis classified as a distant metastasis

Materials and methods

Patients

The institutional review board approved this retrospective study. Written informed consent was obtained from each patient before treatment planning.

We evaluated the GTVs in 21 adenocarcinoma patients who underwent radiation treatment planning for pancreatic cancer using CE-4DCT between September 2014 and June 2016. Patients who had FDG accumulations for whole pancreas due to inflammation were excluded because we were not able to detect the tumors on their 3D-PET/CT images. Patient and tumor characteristics are listed in Table 1. The tumors were located at the pancreatic head in 18 patients and at the pancreatic body in three patients. Two patients had clinically positive lymph nodes (LNs). The median interval of the data acquisition form 3D-PET/CT to CE-4DCT was 10 days (range, 0–40 days).

Data acquisition of CE-4DCT

Imaging parameters of CE-4DCT are listed in Table 2. Patients were positioned in the supine position with arms positioned above the head. CE-4DCT images were acquired under free breathing without breath coaching. The respiratory motion was monitored using a Real-time Position Management™ system (Varian Medical Systems). The intravenous contrast medium was infused at an injection rate of 2 mL/s to scan arterial phases for the planning CT and venous phases for the CE-4DCT. The slice thickness of the CE-4DCT scan was 2 mm. The CE-4DCT images were binned into ten respiratory phases, and all respiratory phases were imported to a radiation treatment planning system (Eclipse™ v11.0; Varian Medical Systems, Palo Alto, CA, USA). Fiducial markers were not used.

Table 2 Imaging parameters of CE-4DCT and 3D-PET/CT

	CE-4DCT	3D-PET/CT
Position of patients	Supine	Supine
Position of arms	Above the head	Above the head
Breath	Free breathing	Free breathing
Breath coaching	None	None
Intravenous contrast medium	Infused at an injection rate of 2 mL/s to scan arterial phases for the planning CT and venous phases for the CE-4DCT	None
Slice thickness (mm)	2	5
FOV (mm)	500	700

SUVmax a maximum standardized uptake value

Data acquisition of 3D-PET

We used the existing diagnostic 3D-PET/CT images for this study. Imaging parameters of 3D-PET/CT are listed in Table 2. Patients were instructed to fast for at least 5 h before the PET imaging. Whole body PET images were acquired under free breathing 90 min after intravenous injection of 3.7 MBq/kg of ^{18}F-FDG. Plain CT images were obtained for attenuation corrections of the PET images. In this study, the 3D-PET/CT images were imported to a radiation treatment planning system (Eclipse™ v11.0).

Delineation of GTV

Concerning inter-observer variations, two radiation oncologists as observers 1 (S.T.) and 2 (M.A.) individually delineated the GTVs on CE-4DCT images at all respiratory phases without any propagated contours from different phases referring to diagnostic 3D-PET/CT images. The two observers also referred to the magnetic resonance (MR) images if available. Diagnostic images were not matched with the CE-4DCT images. Highly suggestive appearances of the extrapancreatic invasions such as peripancreatic strand or coarse reticular structures continuous with the primary lesions [6, 7] were included in the GTVs. As for the two patients with clinically positive LNs, the primary tumor was only used as the GTV in the present study. The sum of the GTV contours from all respiratory phases was used as the GTV-4DCT. Contouring images of all respiratory phases for the GTV-4DCT are shown in Fig. 1.

The 3D-PET/CT images were rigidly coregistered with the planning CT images. Our radiation treatment planning system (Eclipse™ v11.0) was not able to show the standardized uptake value (SUV) in the contouring section, and we were not able to use the threshold value based on the SUV. Therefore, the GTVs on the 3D-PET images were extracted with three thresholds: 20%, 30%, and 40% of maximum activity concentration (GTV-*n*%). Contouring images of the GTV-20%, -30%, and -40% are shown in Fig. 1.

We did not use the threshold of 50% because the GTV-50% was smaller than the GTV-40%, which was obtained from all patients. We did not use the threshold of 10% because the GTV-10% was not obtained from most patients due to the difficulty to distinguish the boundaries between the tumors and the surrounding normal organs on 3D-PET images.

For each of the areas of the primary lesion identified in the first step, GTV-*n*% was defined using an automatic threshold of the maximum activity concentration of the lesion. We selected one of the GTV-*n*%, which mostly resembled the GTV-4DCT in size, as the GTV-PET.

Statistics

The differences between these GTVs were analyzed using Wilcoxon's rank-sum test. We also evaluated the differences of maximum diameters in the left–right (LR), anterior–posterior (AP), and craniocaudal (CC) directions between the GTV-4DCT and GTV-PET using Wilcoxon's rank-sum test. Statistical significance was defined as $p < 0.05$ (two-sided). The software program JMP 11 (SAS Institute, Cary, NC) was used for statistical analyses.

Results

The GTV-20% in 13 patients and the GTV-30% in 10 patients were not obtained because it was difficult to distinguish the boundaries between the tumors and the surrounding normal organs on 3D-PET images. The GTV-20% and -30% were obtained from all of the patients who had tumors with a maximum SUV (SUVmax) ≥ 7.6 and ≥ 6.3,

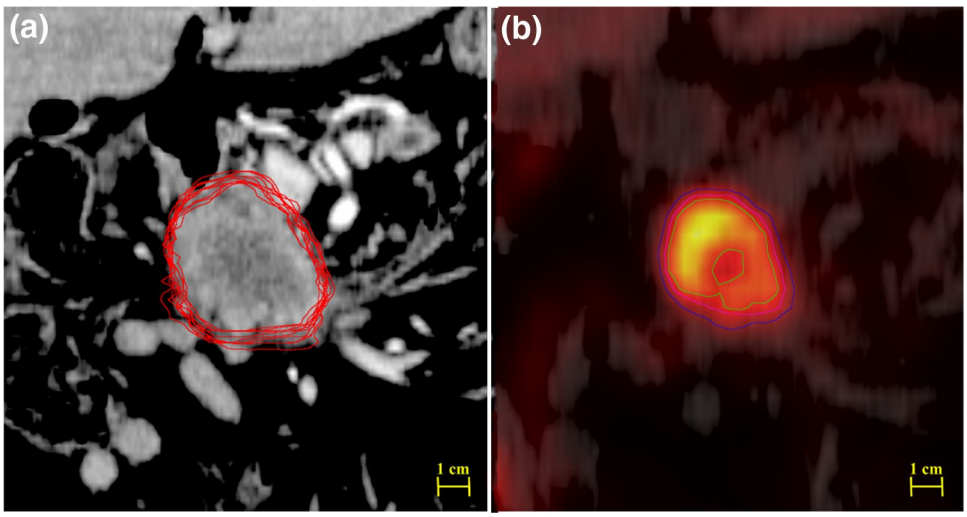

Fig. 1 Contouring images of the GTVs on a coronal plane. **a** Red lines indicate the GTVs contoured from all respiratory phases of CE-4DCT images. Sum of the GTVs contoured from all respiratory phases was used as the GTV-4DCT. **b** Blue, pink, and green lines indicate the GTV-20%, -30%, and -40% on the 3D-PET/CT images, respectively. In this case, the GTV-20% was selected as the GTV-PET, mostly resembles the GTV-4DCT in size among the GTV-*n*%

respectively, which were described on their diagnostic reports. The GTV-40% was obtained from all patients. The GTV-PET consisted of the GTV-20% in eight, -30% in three, and -40% in 10 patients.

Boxplots of the values of the GTVs are shown in Fig. 2. Between observers 1 and 2, there was no significant difference for the values of the GTV-4DCT ($p = 0.53$). The GTV-20%, -30%, -40%, and -PET were significantly smaller than the GTV-4DCT for observers 1 and 2 ($p < 0.01$ each).

Boxplots of the values of maximum diameters in the LR, AP, and CC directions of the GTVs are shown in Fig. 3. Between observers 1 and 2, there was no significant difference for the values of maximum diameters of the GTV-4DCT in the LR, AP, and CC directions ($p = 0.29$, 0.75, and 0.80, respectively). Maximum diameters in the LR, AP, and CC directions of the GTV-PET were significantly smaller than those of the GTV-4DCT for observers 1 and 2 ($p < 0.01$ each). The differences of the median values of maximum diameters between the GTV-4DCT and GTV-PET were 1.7–1.8 cm, 1.4–1.6 cm, and 1.9–2.1 cm in the LR, AP, and CC directions, respectively.

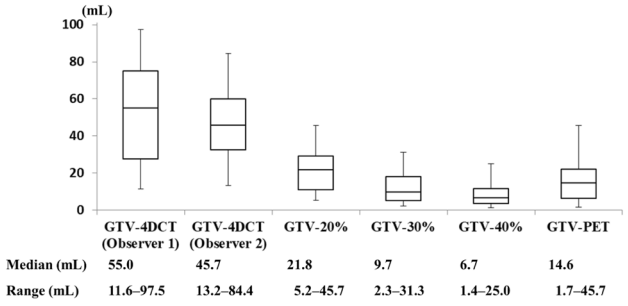

Fig. 2 Boxplots of the values of the GTVs. Center lines, boxes, and error bars indicate median, interquartile range, and maximum or minimum, respectively. GTV-20% in 13 patients and GTV-30% in 10 patients were not obtained because it was difficult to distinguish the boundaries between the tumors and the surrounding normal organs on 3D-PET images. Between observers 1 and 2, there was no significant difference for the values of the GTV-4DCT ($p = 0.53$). The GTV-20%, -30%, -40%, and -PET were significantly smaller than the GTV-4DCT for observers 1 and 2 ($p < 0.01$ each)

Discussion

As the volumes include the respiratory motion, we conducted the present study to assess the differences in the GTVs for pancreatic cancer between 3D-PET and CE-4DCT with all respiratory phases. The GTV-PET based on the 3D-PET images was smaller than the GTV-4DCT for both observers. This result was similar to that of the study conducted by Dalah et al. using 3D-PET and 4DCT [5]. In the study that compared 3D-PET with 4D-PET, the average of target volumes based on the 4D-PET images was 1.6-fold greater than those based on the 3D-PET images [4]. We hypothesize that the GTV based on the 4D-PET images may be more similar to the GTV-4DCT than that based on the 3D-PET images. Further investigations to compare the GTV based on the 4D-PET with the GTV-4DCT are needed.

In our study, highly suggestive appearances of the extrapancreatic invasions such as peripancreatic strand or coarse reticular structures continuous with the primary lesions [6, 7] were included in the GTV-4DCT. To detect pancreatic cancer on the 3D-PET images, a certain number of tumor cells are required [8]. Perhaps the tumor cells in the highly suggestive areas of the extrapancreatic invasions might be inadequate to detect on 3D-PET images. On the other hand, the loss of accuracy of PET related to the low metabolic rates

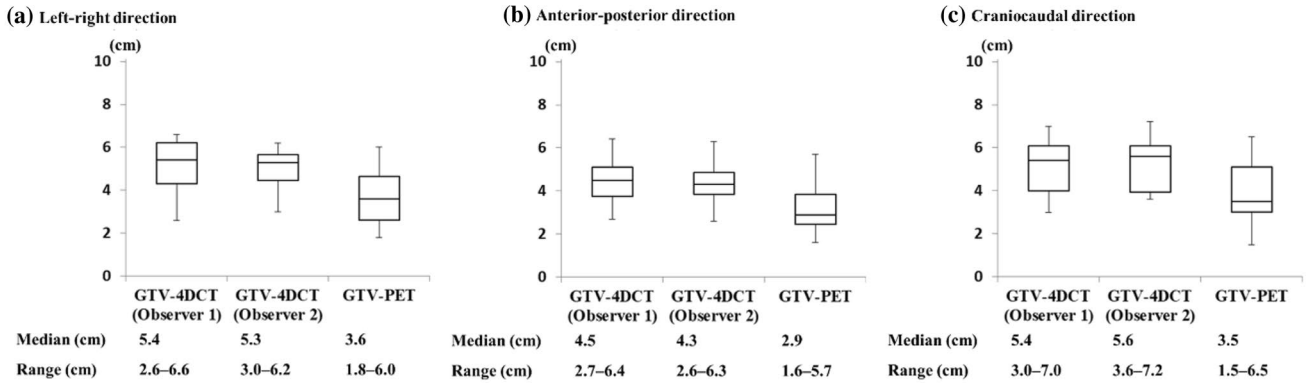

Fig. 3 Boxplots of the values of maximum diameters in the **a** LR, **b** AP, and **c** CC directions of the GTVs. Center lines, boxes, and error bars indicate median, interquartile range, and maximum or minimum, respectively. Between observers 1 and 2, there was no significant difference for the values of maximum diameters of the GTV-4DCT in the LR, AP, and CC directions ($p = 0.29$, 0.75, and 0.80, respectively). Maximum diameters in the LR, AP, and CC directions of the GTV-PET were significantly smaller than those of the GTV-4DCT for observers 1 and 2 ($p < 0.01$ each)

in portions of larger tumors has been reported [1]. Therefore, the GTV-PET in our study might be underestimated.

In the present study, the differences of the median values of maximum diameters between the GTV-4DCT and GTV-PET were 1.7–1.8 cm, 1.4–1.6 cm, and 1.9–2.1 cm in the LR, AP, and CC directions, respectively. Pancreatic cancer spreads irregularly [9], and it was difficult to determine the three-dimensional uniform margin from the GTV-PET to GTV-4DCT.

The present study had several limitations. The inter-observer delineation uncertainty of the GTV was reported in pancreatic cancer [10]. In our study, two radiation oncologists individually delineated the GTV-4DCT as observers 1 and 2 to reduce the influence of the inter-observer variations as much as possible. Between observers 1 and 2, there were no significant differences for the values of the GTV-4DCT and for the values of maximum diameters of the GTV-4DCT in the LR, AP, and CC directions. However, there is still a major limitation due to the inter-observer variation; a systematic review showed that the median was seven observers to test the inter-observer variation [11].

In the radiation treatment planning of pancreatic cancer, an SUV of 2.5 has been known as the threshold of FDG PET [5]. However, our radiation treatment planning system was not able to show the SUV in the contouring section, and we were not able to use the threshold value based on the SUV.

Dalah et al. conducted a study using not only the images of 3D-PET and 4DCT but also the pathologic specimens and the MR images [5]. In our study, the GTVs were not compared with the pathologic specimens because we conducted the present study to assess the differences in the GTVs including the respiratory motion. Moreover, we did not compare the MR images to the 3D-PET and CE-4DCT images because routinely using MR imaging has been difficult due to limited machine resources.

The present study had other limitations in addition to the above mentioned. The sample size was small. The CE-4DCT scans were acquired over a few minutes and were, therefore, not comprehensive enough to capture all the random variations. The interval of the data acquisition from 3D-PET/CT to CE-4DCT was various, and the interval might make some differences on the size of the GTVs.

In conclusion, the GTV-PET based on 3D-PET images was smaller than the GTV-4DCT for pancreatic cancer. When we refer to 3D-PET images without CE-4DCT images, we need to pay attention to the above-mentioned finding to contour the GTV.

Acknowledgements This study was supported by JSPS KAKENHI (Grant number 15K19798).

Compliance with ethical standards

Conflict of interest The authors declare that they have no conflict of interest.

Ethical statement All applicable institutional and national guidelines for the care were followed.

References

1. Kalra MK, Maher MM, Boland GW, Saini S, Fischman AJ. Correlation of positron emission tomography and CT in evaluating pancreatic tumors: technical and clinical implications. Am J Roentgenol. 2003;181:387–93.
2. Ford EC, Herman J, Yorke E, Wahl RL. 18F-FDG PET/CT for image-guided and intensity-modulated radiotherapy. J Nucl Med. 2009;50:1655–65.
3. Callahan J, Kron T, Schneider-Kolsky M, Hicks RJ. The clinical significance and management of lesion motion due to respiration during PET/CT scanning. Cancer Imaging. 2011;11:224–36.
4. Kishi T, Matsuo Y, Nakamura A, Nakamoto Y, Itasaka S, Mizowaki T, et al. Comparative evaluation of respiratory-gated and ungated FDG-PET for target volume definition in radiotherapy treatment planning for pancreatic cancer. Radiother Oncol. 2016;120:217–21.
5. Dalah E, Moraru I, Paulson E, Erickson B, Li XA. Variability of target and normal structure delineation using multimodality imaging for radiation therapy of pancreatic cancer. Int J Radiat Oncol Biol Phys. 2014;89:633–40.
6. Mochizuki K, Gabata T, Kozaka K, Hattori Y, Zen Y, Kitagawa H, et al. MDCT findings of extrapancreatic nerve plexus invasion by pancreas head carcinoma: correlation with en bloc pathological specimens and diagnostic accuracy. Eur Radiol. 2010;20:1757–67.
7. Matsumoto S, Mori H, Kiyonaga M, Sai M, Yamada Y, Hijiya N, et al. "Peripancreatic strands appearance" in pancreatic body and tail carcinoma: evaluation by multi-detector CT with pathological correlation. Abdom Imaging. 2012;37:602–8.
8. Ruf J, Amthauer H, Oettle H, Steinmüller T, Plotkin M, Pelzer U, et al. Role of F18-FDG PET for monitoring of radiochemotherapy—estimation of detectable number of tumour cells. Onkologie. 2004;27:287–90.
9. Deshmukh SD, Willmann JK, Jeffrey RB. Pathways of extrapancreatic perineural invasion by pancreatic adenocarcinoma: evaluation with 3D volume-rendered MDCT imaging. Am J Roentgenol. 2010;194:668–74.
10. Versteijne E, Gurney-Champion OJ, van der Horst A, Lens E, Kolff MW, Buijsen J, et al. Considerable interobserver variation in delineation of pancreatic cancer on 3DCT and 4DCT: a multi-institutional study. Radiat Oncol. 2017;12:58.
11. Vinod SK, Jameson MG, Min M, Holloway LC. Uncertainties in volume delineation in radiation oncology: a systematic review and recommendations for future studies. Radiother Oncol. 2016;121:169–79.